Colloid Polym Sci (2006) 284: 853–861
DOI 10.1007/s00396-005-1444-9

ORIGINAL CONTRIBUTION

Shailesh N. Sharma

Photoinduced charge transfer mechanism in PPV [poly(*p*-phenylinevinylene)] polymer: role of iodide species

Received: 17 August 2005
Accepted: 29 October 2005
Published online: 4 February 2006

S. N. Sharma (✉)
Radiation Laboratory,
University of Notre Dame,
Notre Dame, IN 46556, USA
e-mail: shailesh@mail.nplindia.ernet.in
Tel.: +91-11-25742609
Fax: +91-11-25726938

Present address:
S. N. Sharma
Electronic Materials Division,
National Physical Laboratory,
Dr. K.S. Krishnan Marg,
New Delhi 110012, India

Abstract The photophysical and photochemical behavior of poly (*p*-phenylinevinylene (PPV) polymers in different solvents (toluene and Triton X-100) and in thin form [PPV/optical transparent electrode (OTE)] has been investigated by emission and transient absorption spectroscopies. The absorption and emission studies strongly indicate the presence of dynamic quenching for PPV polymers in different solvents (toluene and Triton X-100) in the presence of LiI/I_2. The fluorescence quenching of the PPV polymer by iodide obeys the linear Stern–Volmer equation for PPV/toluene/LiI system. The positive deviation from Stern–Volmer observed in PPV/Triton X-100/I_2 system may be accounted for by the "quenching sphere of action model". Emission studies indicated an increased conjugation length for PPV polymers on going from solution to the solid state. The emission of PPV was readily quenched by hole scavengers such as I^- (LiI, I_2). The photoinduced charge transfer to these hole scavengers was studied by laser flash photolysis. The transient absorption measurements confirm the formation of I^- and subsequent formation of I_2^{*-} which has been reported for the first time for PPV/I_2 system.

Keywords PPV polymer · Iodide species · Emission spectroscopy · Transient absorption spectroscopy · Static quenching · Dynamic quenching

Introduction

The optical properties of conjugated polymers have been of considerable interest in the past few years, since the discovery of electroluminescence from poly(*p*-phenylinevinylene (PPV) in a light-emitting diode (LED) structure [1]. An important feature of these materials is that their properties can be tuned by chemical modification [2]. When it is made functional with flexible side groups, these materials become soluble in common organic solvents and can be solution-processed at room temperature into uniform, large-area, optical-quality thin films. Such films are flexible and easily fabricated into desired shapes that are useful in novel devices [2, 3]. The ease of polymer processing compared to conventional inorganic semiconductors offers the potential for enormous cost savings in applications that require visible band-gap semiconductors. Thus, conjugated polymers offer the possibility for completely new applications such as cost-effective, large-area, luminescent panels and flexible, lightweight display devices [4, 5]. At present, PPV and several alkoxy- and cyano-substituted derivatives of PPV are being used to develop both higher efficiency LEDs and structures that have emission over different ranges of the visible spectrum [6]. The discovery that their photoluminescence and electroluminescence spectra are essentially identical suggests that the state from which emission occurs is the same in both cases [3, 7]. Hence, a great deal of attention has been devoted to the understanding of the fundamental photophysical process underlying the emission.

The key issue for control of color and efficiency of light emission depends upon the length of the conjugated segments of PPV and its derivatives. Furthermore, the efficiency of luminescence was shown to be significantly

enhanced, when isolation of short conjugated segments is achieved, because of excitation confinement [8]. The various methods used to control the conjugation length of PPV and its derivatives are: temperature of elimination, selective elimination, and controlled oxidation approaches [9–11]. For this reason, PPV is a very suitable material to use in studying the influence of conjugation length on electronic properties [8]. The PPV films used in this study were prepared from *p*-xylenebis (tetrahydrothiophenium chloride) precursor. These precursor films were thermally converted in a vacuum in a temperature-controlled oven.

Despite the large variety of potential applications, optimizing the performance characteristics of conjugated, polymer-based devices is complicated by the molecular nature of these materials. Variations in how a conjugated polymer is processed can alter the way in which the polymer chains pack together which in turn, affect the bulk electronic properties of conjugated polymer films. The primary effect comes from the fact that conjugated polymer chains take on different conformations in different solution environments [12, 13]. Thus, the film morphology and the performance of conjugated polymer-based devices can be controlled by a number of solution-processing factors, including changing either the solvent or the concentration of the solution from which the polymer film is cast [13, 14]. Thus, to understand better the photophysical processes of PPV, detailed fluorescent studies of PPV both in solution (in different solvents—aromatic and aliphatic) and in thin film form have been studied. Conductor and semiconductor polymers particularly have many doping possibilities for specific applications [15]. It is known that iodine-doping results in the formation of charge transfer complexes [16]. It has also been shown that iodine can improve the performance of light emitting diodes [17]. Thus, it appears that iodine is the most promising dopant because it does not induce any degradation of the polymer used to realize organic light emitting diodes [17]. For this reason, many experiments were carried out using iodine and lithium iodide as a dopant. In the present work, the charge transfer mechanism between the polymer (PPV) and the dopant (lithium iodide) has been monitored by using nanosecond laser flash transient absorption spectroscopy and has been reported for the first time.

Experimental section

Materials and methods

The materials used were of the purest quality available and used as received. Absorption spectra were recorded using Shimadzu 3100PC Spectrophotometer. Steady state emission spectra were recorded using an SLM-Aminco 8100 spectrofluorometer. The quantum-yield values were determined using Rhodamine 6G solution as reference. Time-resolved absorption experiments (Nanosecond Laser Flash Photolysis) were performed using a Quanta-Ray Nd-YAG laser system (355 nm, pulse width ~6 ns, 5 mJ). A typical experiment consisted of a series of three to six replicate shots at a single monitoring wavelength. The photomultiplier output was digitized with a Tektronix 7912 AD programmable digitizer. The signals from the photomultiplier were processed by a LSI-11 microprocessor interfaced with a VAX computer. Cutoff filters were used to avoid spurious responses from second-order scattering from the monochromator gratings. The details of the experimental setup can be found elsewhere [18].

Synthesis of precursor-PPV

PPVs are normally synthesized by two methods: precursor route and direct solution polymerization for organic soluble polymers [19–21]. Among the methods investigated, the precursor route is very simple and can normally result in polymers with high molecular weights and high structural regularity. In precursor route, a commercially available monomer (*p*-xylenebis) is polymerized with a NaOH base to yield a sulphonium salt polyelectrolyte precursor polymer. The precursor polymer is converted to standard PPV by heat treatment in vacuum at temperatures of typically 220°C [21].

In a typical experiment, 5.6 ml of ice-cold, N_2-purged dry-methanolic NaOH solution (0.57 gm in 5.6 ml of methanol) was added in a slow stream to an ice-cold, N_2-purged, dry-methanolic solution of the *p*-xylenebis (tetrahydrothiophenium chloride) monomer (4 gm in 30 ml of methanol). The resulting mixture was stirred for 2 h at real time under inert atmosphere; the polymer that precipitated out was isolated, washed with methanol, filtered, and redissolved in tetrahydrofuran (THF). The THF solution was then filtered, concentrated, and the polymer precipitated from methanol. The process of dissolution and re-precipitation was repeated four times to get rid of low molecular weight acidic impurities. The polymer was then dried at 65°C in vacuum for 1 h and at 220°C for an additional 5 h. The PPV-polymer then obtained was suspended in various solvents (toluene and Triton X-100) for absorption and emission measurements.

Preparation of PPV thin film

A small amount of PPV polymer (usually 1 ml) suspension in toluene (1%) was applied to the conducting surface of 0.8×5 cm^2 optical transparent electrode (OTE) and was

dried in air on a warm plate. The PPV-polymer-coated OTE was then given heat treatment in vacuum for ~6 h. The PPV thin film on OTE would be referred as PPV/OTE thin film.

Results and discussion

To understand the photophysical process of the PPV polymer, lithium iodide in acetonitrile was used as dopant. The absorption spectra of PPV in toluene, of LiI in acetonitrile solution, and PPV-LiI in solution are shown in Fig. 1a. In the spectrum of pure PPV (Fig. 1a, curve a), there is a major broad peak centered at 500 nm. In the spectrum of pure LiI in acetonitrile, there is a strong absorption in the ultraviolet at wavelengths ~360 nm (Fig. 1a, curve b), whereas the absorption in the visible is relatively weak (at 500 nm, the LiI absorption is weak compared with that from PPV at the same concentration). No indication of a spectral shift is observed as the LiI is added. For the mixture of PPV and LiI, at the LiI concentration of 20 and 40 mM, the absorption spectrum (Fig. 1a, curves c and d) is simply a superposition of the PPV and LiI absorption spectra (Fig. 1a, curves a and b). Figure 1b shows the effect of LiI concentration on the emission intensity of PPV polymer. The peak of emission of PPV in toluene is at about 516 nm with a shoulder at about 550 nm (Fig. 1b). The details of the system, quencher, and its concentration, along with its emission and quantum yield values, are summarized in Table 1. It is evident from Fig. 1b (curves a–f) that with an increase in LiI concentration from 0 to 27 mM, the emission intensity is decreased considerably with corresponding quantum yields being Φ~0.3 and 0.029 (Table 1), respectively, which implied that fluoroscence quenching of PPV was only due to LiI. The hole scavengers such as I^- quenched the PPV emission as these anions reacted with the photogenerated holes.

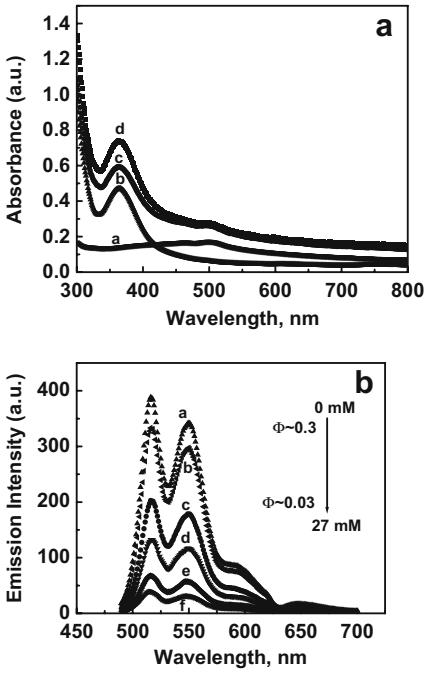

Fig. 1 **a** Absorption spectra of *a* PPV (60 mM), *b* LiI (60 mM), *c* mixture of PPV and LiI (20 mM), and *d* mixture of PPV and LiI (40 mM). **b** Emission spectra of PPV polymer for different concentrations of LiI: *a* 0, *b* 0.7, *c* 3.4, *d* 7.0, *e* 13.4, and *f* 27 mM. Emission spectra were recorded using 440-nm excitation. The PPV polymer and LiI are suspended in toluene and acetonitrile, respectively

Fluorescence quenching refers to any process that decreases the fluorescence intensity of a sample. There are a wide variety of quenching processes that include excited state reactions, molecular rearrangements, ground state complex formation, and energy transfer [22–24]. Quenching experiments can be used to determine the accessibility of a quencher to a fluorophore, monitor conformational changes, and monitor association reactions of the fluorescence of one of the reactant changes upon binding. There are two basic types of quenching: static and dynamic (collisional). Both types require an interaction between the fluorophore and quencher. In the case of dynamic quenching, the quencher must diffuse to the fluorophore during the lifetime of the excited state. Upon contact, the fluorophore returns to the ground state without emission of a photon [22]. In the case of static quenching, a complex forms between the fluorophore and the quencher and this complex is nonfluorescent. The formation of this complex does not rely upon the population of the excited state [22]. We will consider them independently.

Table 1 Details of the system, quencher, and its concentration with the experimental values of emission maximum (nm) and quantum yield

System	Quencher	[*Q*] mM	Emission, $\lambda_{max.}$(nm)	Quantum yield[a]
PPV/toluene	LiI	0	516	0.3
PPV/toluene	LiI	0.7	516	0.25
PPV/toluene	LiI	3.4	516	0.156
PPV/toluene	LiI	7.0	516	0.102
PPV/toluene	LiI	13.4	516	0.051
PPV/toluene	LiI	27.0	516	0.03
PPV/triton X-100	I_2	0	510	0.2
PPV/triton X-100	I_2	0.025	510	0.19
PPV/triton X-100	I_2	0.05	510	0.185
PPV/triton X-100	I_2	0.1	510	0.1705
PPV/triton X-100	I_2	0.2	510	0.123
PPV/triton X-100	I_2	0.3	509	0.079
PPV/triton X-100	I_2	0.4	510	0.0527
PPV/triton X-100	I_2	0.5	510	0.0348
PPV/triton X-100	I_2	0.6	510	0.0225

[a]Determined using Rhodamine 6G solution as reference

Collisional (dynamic) quenching

Collisional quenching occurs when the excited-state fluorophore is deactivated by contact with some other molecule in a solution, which is called the quencher. The molecules are not chemically altered in the process. For collisional quenching, the decrease in intensity is described by the ratio of the fluorescence in the absence of quenching to the presence of quencher by the Stern–Volmer equation [22]:

$$I_o/I = 1 + k_q\tau_o[I^-] = 1 + K_{SV}[I^-] \quad (1)$$

where I_o and I are the emission intensities of PPV in the absence and presence of iodine (quencher), respectively. k_q is the bimolecular quenching constant and τ_o (as determined from lifetime measurements, ~0.5 ns) is the lifetime of PPV polymer in the absence of iodine and $K_{SV}=k_q\tau_o$ is the Stern–Volmer quenching constant. From the slope ($K_{SV}=k_q\tau_o$) of this plot (Fig. 2), we obtain a Stern–Volmer quenching constant (K_{SV}) ~348 M^{-1} and quenching rate constant (k_q) of ~7×10^{11} M^{-1} s^{-1}. The straight line plot of I_o/I vs the iodide concentration (Fig. 2) confirms the presence of dynamic quenching.

Static quenching

It involves the formation of a complex between the quencher and fluorophore that does not rely on diffusion in the excited state. Static quenching like dynamic quenching also gives a linear Stern–Volmer plot [22].

In the simplest case for static quenching,

$$I_o/I = 1 + K_S[Q] \quad (2)$$

where K_S is the static quenching constant. Here, the dependence of I_o/I on [Q] is also linear and is very similar to that observed for dynamic quenching except that the quenching constant is now the association constant of the complex. Thus, at low quencher concentrations, the dependences of fluorescence quenching on the quencher concentration for the two processes are identical. From above, it is clear that the fluorescence-quenching data alone cannot distinguish between dynamic or static processes. Additional information is required to distinguish between the two; for example, absorption spectra and the lifetime dependence. In dynamic quenching, charge transfer occurs and the fluorescence is quenched when the electron acceptor collides with the excited fluorophore. By careful examination of the absorption spectrum, one can attempt to distinguish static and dynamic quenching. Because the collision between the quencher and the fluorophore affects only the excited state of the fluorophore, no changes in the absorption spectrum are expected [22, 25]. On the contrary, the formation of ground-state complex in static quenching will perturb the absorption spectra of the fluorophore [22, 25]. Figure 1a clearly shows that the absorption spectrum of the mixture is a linear combination of the spectra of each component, thus implying the presence of dynamic quenching. The data are consistent with the results of Min Zheng et al. [26] even at the very high concentration of of C60 in MEH-PPV mixture; they found neither spectral shift nor any new absorption band due to the complex formation.

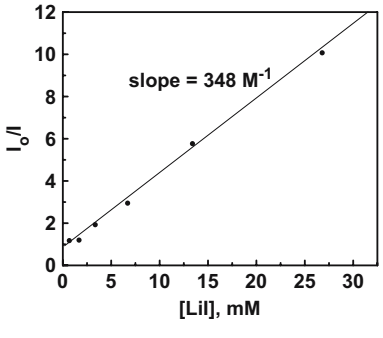

Fig. 2 Stern–Volmer plot of PPV/LiI system showing the dependence of I_o/I on the concentration of LiI

Also, in the case of purely collisional (dynamic) quenching, the Stern–Volmer equation can also be written as:

$$I_o/I = \tau_o/\tau \quad (3)$$

where τ and τ_o are the excited state lifetimes in the presence and absence of quencher, respectively [22].

Hence, in this case, from Eq. 1,

$$\tau_o/\tau = 1 + K_{SV}[I^-] \quad (4)$$

On substituting the values of τ_o ~0.5 ns, K_{SV} ~348 M^{-1}, and [I^-] ~27 mM, we get τ ~0.048 ns which indicates that in the presence of the quencher [I^-], the excited state lifetime has been reduced from 0.5 to ~0.05 ns which was also observed experimentally. In the case of static quenching, the lifetime of the sample will not be reduced because those fluorophores which are not complexed and are able to emit after excitation will have normal, excited state properties. The fluorescence of the sample is reduced as the quencher is essentially reducing the number of fluorophores which can emit. This reduction in the lifetime of the excited species (fluorophore-PPV) upon the addition of the quencher (I^-) further demonstrates the absence of static quenching and the presence of only dynamic quenching for PPV/toluene/LiI system.

Figure 3 shows the absorption and fluorescent spectra of PPV polymer in Triton X-100/Di–H_2O solvent. As shown in Fig. 3a (curve a), the PPV absorption in the absence of I_2 shows a band ~505 nm but upon increasing the concentration of I_2 from 0 to 0.3 mM, the absorption features corresponding to iodide at ~370 nm develops concomi-

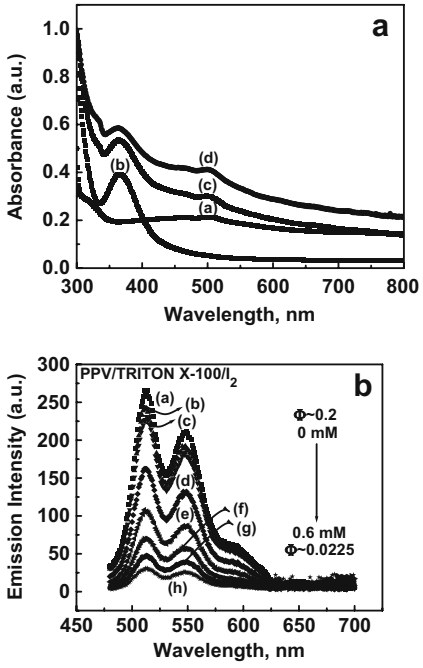

Fig. 3 **a** Absorption spectra of *a* PPV, *b* I_2, and *c* mixture of PPV and I_2 (0.3 mM). **b** Emission spectra of PPV polymer for different concentrations of I_2: *a* 0, *b* 0.05, *c* 0.1, *d* 0.2, *e* 0.3, *f* 0.4, *g* 0.5, and *h* 0.6 mM. Emission spectra were recorded using 440-nm excitation. The PPV polymer and I_2 are suspended in Triton X-100 and acetonitrile, respectively

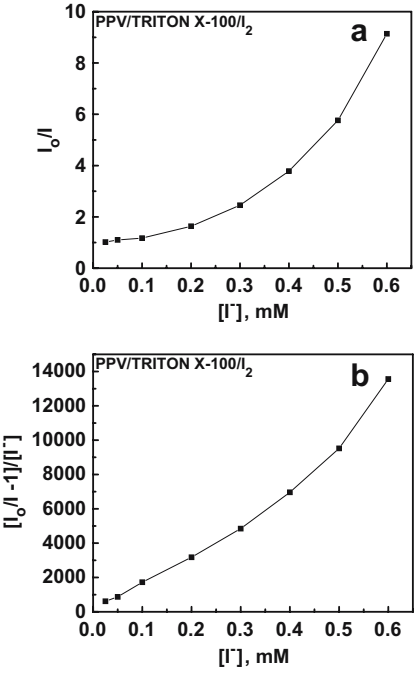

Fig. 4 **a** Stern–Volmer plot showing the dependence of I_o/I on the concentration of I_2. **b** Modified Stern–Volmer plot of PPV/Triton X-100/I_2 system

tantly as evident from Fig. 3a (curve c). As in the case of PPV/toluene/LiI system, here the absorption curve [Fig. 3a (curve c)] is merely a superposition of the individual absorption spectra of PPV/Triton X-100 and I_2, respectively. Figure 3b shows the emission intensity profiles of PPV/Triton X-100 system which exhibits main peak at ~510 nm with a shoulder ~550 nm similar to that of PPV/toluene system. From Fig. 3b and Table 1, it is evident that with increase in I_2 concentration from 0 to 0.6 mM, the emission intensity is decreased considerably with corresponding quantum yields being Φ~0.2 and 0.0225, respectively. From the absorption and emission trend of PPV/Triton X-100/I_2 system, it is evident that dynamic quenching is dominant as in the case of PPV/toluene/LiI system. However, as shown in Fig. 4a, the Stern–Volmer plot of the relative intensity is nonlinear with an upper curvature which may indicate the presence of a static quenching coupled with a diffusion transient effect [22, 26, 27]. When both dynamic and static fluorescence quenching occur together, then a modified form of the Stern–Volmer equation is used and is given as:

$$I_o/I = (1 + K_{SV}[Q])(1 + K_a[Q]) \tag{5}$$

where K_{SV} and K_a are constants associated with dynamic and static quenching, respectively [22, 26]. In the absence of fluorescence lifetime data for PPV/Triton X-100/I_2 system, Eq. 5 can be modified to resolve both the static and dynamic components. The expansion of the parentheses of Eq. 5 yields:

$$I_o/I = 1 + (K_{SV} + K_S)[Q] + K_{SV}K_S[Q]^2 \tag{6}$$

$$I_o/I = 1 + K_{APP}[Q] \tag{7}$$

where

$$K_{APP} = (I_o/I - 1)/[Q] = (K_{SV} + K_S) + K_{SV}K_S[Q] \tag{8}$$

In this study, K_{APP} is the apparent quenching constant and is typically calculated at each quencher concentration. Then, a plot of K_{APP} vs [*Q*] should give a straight line with an intercept *I* of K_{SV}+K_S and a gradient *G* of $K_{SV}K_S$. However, from the plot as shown in Fig. 4b, linearity is observed only at low concentrations of quencher while an upward curvature is obtained at higher values of [*Q*]. This anomaly can be explained by taking into account the "sphere of action" static quenching model [28]. This is often observed at high quencher concentrations due to the existence of an increasing numbers of quencher-fluoro-

phore pairs in which the quencher is close enough to the fluorophore upon excitation to instantly quench its excited state. In the solution, this critical distance defines an interaction sphere of volume *V*. The probability of the quencher being within this volume at the time of excitation depends on both the quencher concentration and the volume. Then Eq. 5 can be rewritten as:

$$I_o/I = (1 + K_{SV}[Q])e^{V[Q]} \quad (9)$$

The term *V* (static quenching constant) in this equation represents an active volume element around the fluorophore such that any quencher within this volume at the time of fluorophore excitation is able to quench the excited fluorophore [28]. For our PPV/Triton X-100/I_2 system, the Stern–Volmer plot (Fig. 4a) shows a nonlinear behavior which indicates that iodide does not form a ground state complex with PPV/Triton X-100 system as would have happened for pure static quenching process. Rather, at higher concentrations of the quencher (I_2), iodide is in such close proximity to PPV that quenching occurs immediately upon excitation. This process appears as static quenching would in a Stern–Volmer plot. Thus, the deviation from linearity in Stern–Volmer's plot (Fig. 4a) cannot be attributed to the contribution of pure static quenching because there is no formation of ground-state complex as evident from Fig. 4a, nor any change is observed in the absorption spectra of PPV/Triton X-100 (the fluorophore) upon the addition of iodine (the quencher) (Fig. 3a, curve c), but rather due to dynamic quenching due to the presence of a quencher molecule within the quenching sphere of action. This is in accordance as reported by others that the sphere of action static quenching model does not produce changes in the absorption spectrum [26].

From the above results of absorbance and emission of PPV in different solvents (toluene and Triton X-100), it is evident that the dynamic quenching is mainly responsible for the decrease in the emission intensity of PPV upon the addition of LiI/I_2. Also, not much difference in emission maximum (λ_{max}±5) of PPV in different solvents (toluene and Triton X-100) was observed (Table 1). These results are contrary to the earlier reported where a slight redshift of the absorption spectra in aromatic solvents (Triton X-100) compared with that in aliphatic solvents (toluene) is obtained [29]. However, this difference should have been clearer in emission spectra which are narrower and well defined but it is absent. It is known that the absorption spectrum of conjugated polymer depends on its molecular conformation due to the changing conjugation length of the polymer [29]. Thus, it is expected that polymer might have different conjugation length in different solvents [29]. However, from the absorption and emission intensity profiles of PPV in different solvents of toluene and Triton X-100, no such trend is evident. Thus, we believe that our polymer has similar conjugation lengths both in toluene and Triton X-100. Our results are in contrast with the findings of Diaz-Garcia et al. [30] where photophysics of MEH-PPV polymer films cast from different solvents were found to be different.

Figure 5a (curves a–e) shows emission intensity profiles of PPV/OTE films which are exposed to constant I_2 atmosphere for different intervals of time. Here, the main emission peak is ~555 nm with a hump at ~595 nm, respectively. Table 2 summarizes the experimental values of emission and quantum yield of PPV/OTE for different times of exposure to I_2. As evident from Fig. 5a and Table 2, a significant quenching of emission for PPV/OTE films are observed with increment in iodine exposure time with corresponding decrease in emission yield from Φ~0.15 to 0.0055, respectively. On comparing the emission intensity profiles of PPV in various solvents (Table 1) with that of solid state emission spectra (Table 2), it is interesting to note that PPV emission spectra in solid state are significantly redshifted as compared to PPV solution spectra which are almost identical. This is due to the fact that the emitting species for the two polymers are identical in solution but are different in the solid state [31]. A redshift in the emission on going from solution to solid state is commonly observed for polymers and is attributed to increased conjugation length from improved ordering in the solid state [31].

Quenching in PPV/OTE thin films upon addition of I_2 dopant appears to be stronger as compared to their

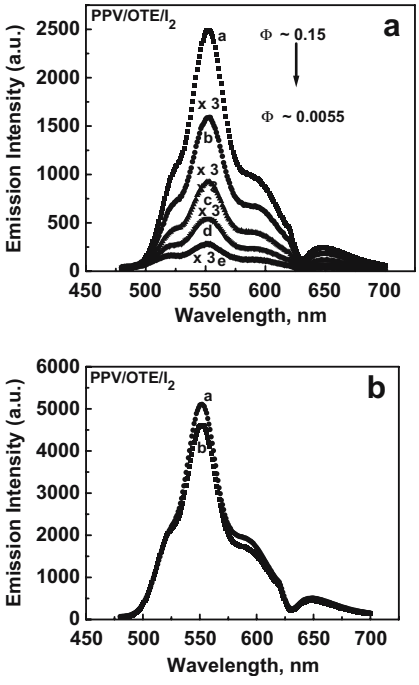

Fig. 5 Emission spectra of PPV/OTE thin films exposed to **a** I_2 atmosphere for different durations: (a) 0, (b) 1, (c) 2, (d) 4, and (e) 8 h, and **b** atmosphere for 7 days. Emission spectra were recorded using 440-nm excitation

Table 2 Experimental values of emission maximum (nm) and quantum yield of PPV/OTE thin films for different times of exposure to I_2

Time of exposure of PPV/OTE to iodine (h)	Emission, $\lambda_{max.}$ (nm)	Quantum yield[a]
0	553	0.15
1	553	0.032
2	553	0.0186
4	553	0.011
8	554	0.0055

[a]Determined using rhodamine 6G solution as reference

counterparts in solution form. This could be due to the fact that PPV has significant crystallinity in the solid state and as a result has the most structured emission spectra with well-defined vibronic features [32]. From the emission intensity profiles of PPV both in toluene and Triton X-100, it has been reported that the shape of the emission spectrum of polymers is determined by the nature of the emitting species and the amount of inhomogeneous broadening [32, 33]. Inhomogeneous broadening is due to the emission from a range of conjugation lengths in the sample, which is not observed in our case.

It has been reported that PPV polymers show signs of rapid photodegradation in the presence of oxygen or moisture [34]. From Fig. 5b, there is only a marginal decrease in emission intensity for our PPV/OTE thin films when exposed to atmosphere for 7 days as compared to as-prepared PPV/OTE thin films. Thus, even without any adequate encapsulation, our PPV/OTE thin films are quite stable and its emission intensity gets quenched only in the presence of iodine atmosphere.

We have found that the emission intensity of PPV both in solution and in thin film form is noticeably modified in the presence of iodine atmosphere. The existing emission peak of pure PPV is suppressed upon the addition of iodine and this can be attributed to nonradiative recombination of excitons at the iodine centers [35]. Luminescence suppression in PPV films after iodine implantation has been already observed and explained in terms of implantation-induced radiation defects serving as quenching centers [36]. It has been reported earlier that iodine doping of polymers results in the formation of strong new luminescent band at ~475 nm which not only suppresses the characteristic luminescence of the host material but also results in considerable short-wavelength shift in the luminescence spectrum [35]. However, in our case, no new band at ~475 nm associated with iodine could be seen and only quenching of fluorescence due to iodine of our PPV polymer both in solution and in thin film form was observed.

It has been reported earlier from X-ray photoelectron spectroscopy studies that iodine doping of polymers results

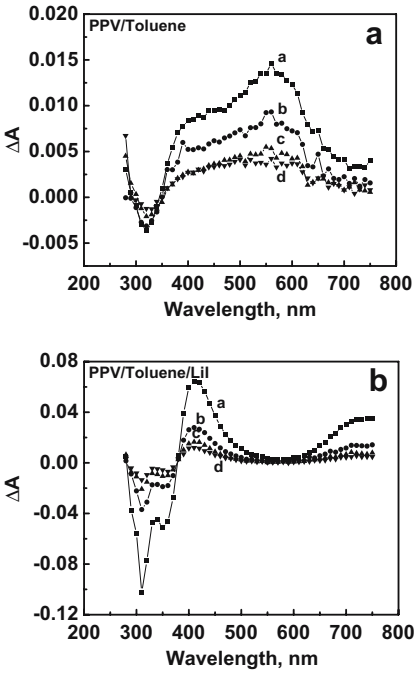

Fig. 6 Transient absorption spectra of PPV polymer suspension in deaerated toluene after 355-nm laser pulse excitation: **a** no added LiI and **b** in the presence of 60.0 mM LiI recorded at different intervals of time, *a* 1, *b* 5, *c* 10, and *d* 15 μs

in the formation of charge-transfer complexes and the presence of anionic species I_5^-/I_3^- has been indicated [37]. If the interaction of excited PPV with iodine results in

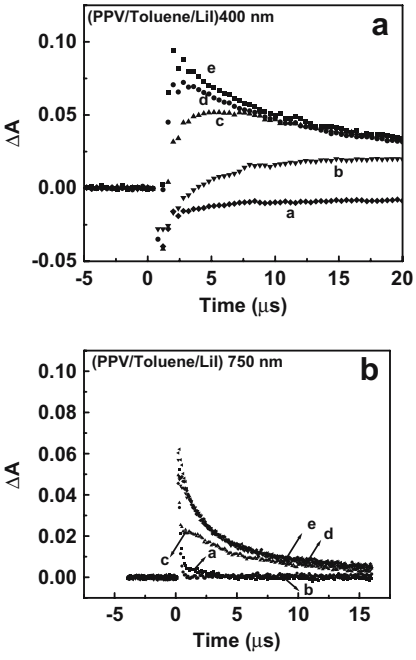

Fig. 7 Absorption–time profile recorded at **a** 400 and **b** 750 nm following the 355-nm laser pulse excitation of PPV polymer in toluene containing *a* 5, *b* 10.0, *c* 20.0, *d* 40.0, and *e* 60.0 mM LiI

charge transfer, then we should be able to monitor charge transfer products using transient absorption spectroscopy. As evident from Fig. 6a, the transient absorption spectra of PPV produced after direct excitation in deaerated toluene shows four bands with absorption maxima at around 340, 400, 550, and 700 nm, respectively. The negative band below 400 nm can be ascribed to the depletion of ground state of PPV. In the transient absorption spectra for M-PPV, Ma et al. [38] attributed the negative band below 450 nm to the depletion of ground state of M-PPV. The band centered at 550 nm might be attributed to triplet–triplet absorption of PPV because this transient was quenched upon admission of air to the PPV/toluene solution [38]. A band at ~640 nm was attributed to the M-PPV radical cation [38]. Thus, the transient signal at around 700 nm can be attributed to PPV-radical cation. Surface adsorbed I^- on the PPV quickly scavenges away the holes from PPV and forms I^*, which then interacts with the adjacent I^- to yield I_2^{*-}.

$$\mathrm{PPV(h)} + \mathrm{I}^- \rightarrow \mathrm{PPV} + \mathrm{I}^* \xrightarrow{\mathrm{I}^-} \mathrm{I}_2^{*-} \tag{10}$$

On a longer time scale, I_2^{*-} will disproportionate to yield two-electron oxidation product I_3^- and I^- (reaction 11).

$$\mathrm{I}_2^{*-} + \mathrm{I}_2^{*-} \rightarrow \mathrm{I}_3^- + \mathrm{I}^- \tag{11}$$

Of the iodide ion oxidation products, I_2^{*-} is the only reaction intermediate detectable in our nanosecond laser-flash photolysis apparatus [39]. The absorption bands observed at 400 and 750 nm confirm the formation of I_2^{*-} [40] (Fig. 6b). To probe the role of PPV/toluene in the oxidation of I^-, the yield of I_2^* radical at various concentrations of LiI was monitored. With increase in concentration of LiI from 0 to 60 mM, an increase in the yield of I_2^{*-} as observed from the increment in absorption at 400 and 750 nm, was observed (Fig. 7a,b). In this study, the charge transfer process between PPV and LiI occurs at a rate of less than 15 μs. This delay in the appearance of the transients at 400 and 750 nm in the laser flash photolysis experiments confirmed the presence of dynamic quenching processes in the formation of I_2^{*-} [40]. This interfacial hole-transfer process is similar to the oxidation of thiocyanate in colloidal TiO_2 [41] and ZnO [42] systems.

Conclusions

The PPV polymer in different solvents and in thin film form exhibits interesting photophysical and photochemical properties. From the Stern–Volmer plots, dynamic quenching has been identified as the basic mechanism for PPV/toluene/LiI and PPV/Triton X-100/I_2 systems, respectively. The nonlinearity (upward curvature) as observed in the Stern–Volmer plot for PPV/Triton X-100/I_2 system (Fig. 4) has been analyzed in terms of sphere of action static quenching model for high values of the concentration of the quencher indicating a close proximity between the fluorophore and the quencher in the excited state. The effect of iodide concentration on the emission spectra of PPV is different for thin films as compared to different solvents because of the different interaction mechanisms. The quenching of the emission of PPV polymer can be used to probe the hole transfer by PPV–iodide complex in the excited state with subsequent formation of I_2^{*-}. This interfacial hole transfer process is completed within the duration of ~15 μs. The results obtained here are meaningful for future applications of polymer-halide fluorescence sensor research.

Acknowledgements The work described herein was supported by the Office of the Basic Energy Sciences of the US Department of Energy. I would like to thank Prof. Prashant Kamat for helpful discussions.

References

1. Burroughes JH, Bradley DDC, Brown AR, Marks RN, Mackay K, Friend RH, Burn PL, Holmes AB (1990) Nature 347:539
2. Braun D, Heeger A (1991) J Appl Phys Lett 58:1982
3. Gustafsson G, Cao Y, Treacy GM, Klavetter F, Colinari N, Heeger AJ (1992) Nature 357:477
4. Bharathan J, Yang Y (1998) Appl Phys Lett 72:2660
5. Hebner TR, Wu CC, Marey D, Lu MH, Strum JC (1998) Appl Phys Lett 72:519
6. Yu G, Wang J, McElvain J, Heeger AJ (1998) Adv Mater 10:1431
7. Brown AR, Greenham NC, Burroughes JH, Bradley DDC, Friend RH, Burn PL, Kraft A, Holmes AB (1992) Chem Phys Lett 200:46
8. Brown AR, Burn PL, Bradley DDC, Friend RH, Kraft A, Holmes AB (1992) Mol Cryst Liq Cryst 216:111
9. Burn PL, Holmes AB, Kraft A, Bradley DDC, Brown AR, Friend RH, Gymer RW (1992) Nature 356:47
10. Burn PL, Holmes AB, Kraft A, Bradley DDC, Brown AR, Friend RH (1992) J Chem Soc Chem Commun 1:32
11. Yu Y, Lee H, Vanlaeken A, Hsieh BR (1998) Macromolecules 31:5553
12. Nguyen TQ, Martini I, Liu J, Schwartz BJ (2000) J Phys Chem B 104:237
13. Wang P, Collison CJ, Rothberg LJ (2001) J Photochem Photobiol A 144:63
14. Lim SH, Bjorklund TG, Bardeen C (2001) J Chem Phys Lett 342:555

15. Nakazawa Y, Hoshino K, Hanna JL, Kokado H (1989) J Appl Phys 28:12517
16. Alimi K, Safoula G, Bernede JC, Rabiller C (1996) J Polym Sci Part B 34:845
17. Huang F, MacDiarmid AG, Hsieh BR (1997) Appl Phys Lett 71:2415
18. Thomas MD, Hug GL (1998) Comput Chem (Oxford) 22:491
19. Burn PL, Bradley DDC, Friend RH, Halliday DA, Holmes AB, Jackson RW, Kraft A (1992) J Chem Soc Perkin Trans 1:3225
20. Pichler K, Halliday DA, Bradley DDC, Burn PL, Friend RH, Holmes AB (1993) J Phys Condens Matter 5:7155
21. Padmanaban G, Ramakrishnan S (2000) J Am Chem Soc 122:2244
22. Lakowicz JR (1999) Principles of fluorescence spectroscopy, 2nd edn. Kluwer-Plenum, New York
23. Pesce AJ, Rosen CG, Pasby TL (eds) (1971) Fluorescence spectroscopy. Marcel Dekker, New York
24. RM Clegg (1996) Fluorescence imaging spectroscopy and microscopy. In: Wang XF, Herman B (eds) Wiley, New York
25. Li Sha-Yu, Xiong Fei, Zhang Hai-Rong, Lu Xue-Fang, Li Yi, Yang Guo-Qiang (2004) Chin J Chem 22:80
26. Min Zheng, Fenglian Bai, Li Fengying, Yuliang Li, Daoben Zhu (1998) J Appl Polym Sci 70:599
27. Keizer J (1983) J Am Chem Soc 105:1494
28. Wang Deli, Wang Jian, Moses Daniel, Bazan Guillermo C, Heeger Alan J (2001) Langmuir 17:1262
29. Zheng M, Bai F, Zhu DJ (1998) Photochem Photobiol A 116:143
30. Diaz-Garcia MA, Hide F, Schwartz BJ, Andersson MR, Pei Q, Heeger AJ (1997) Synth Met 84:455
31. Gettinger CL, Heeger AJ, Drake JM, Pine DJ (1994) J Chem Phys 101:1673
32. Martens JHF (1993) Synth Met 55–57:434
33. Harrison NT, Baigent DR, Samuel IDW, Friend RH, Grimsdale AC, Moratti SC, Holmes AB (1996) Phys Rev B 53:15815
34. Hu B, Karaz FE (1998) Chem Phys 227:263
35. Pope M, Swenberg CE (1999) Electronic processes in organic crystals and polymers. Oxford Science, Oxford
36. Hamer PJ, Pichler K, Harrison MG, Friend RH, Ratier B, Moliton A, Moratti SC, Holmes AB (1996) Phila Mag B 73:367
37. Zaidi B, Ayachi S, Mabrouk A, Molinie P, Alimi K (2003) Polym Degrad Stab 79:183
38. Ma L, Wang X, Wang B, Chen J, Wang J, Huang K, Zhang B, Cao Y, Han Z, Qian S, Yao S (2002) Chem Phys 285:85
39. Bedja I, Kamat PV (1995) J Phys Chem 99:9182
40. Kamat PV (1985) Langmuir 1:608
41. Kamat PV, Patrick B (1991) In: Levy B, Deaton J, Leubner I, Slifkin L, Nuenter A, Kamat PV, Tani T (eds) Proceedings of the 44th IS&T meeting. The Society for Imaging Science and Technology, Springfield, VA, pp 293
42. Brabec CJ, Cravino A, Zerza G, Sariciftci NS, Kiebooms R, Vanderzande D, Hummelen JC (2001) J Phys Chem B 105:1528